JMEPEG (2014) 23:3907–3915
DOI: 10.1007/s11665-014-1205-3

1059-9495/$19.00

Influence of Electropolishing and Magnetoelectropolishing on Corrosion and Biocompatibility of Titanium Implants

Zia ur Rahman, Luis Pompa, and Waseem Haider

(Submitted April 24, 2014; in revised form July 28, 2014; published online August 19, 2014)

Titanium alloys are playing a vital role in the field of biomaterials due to their excellent corrosion resistance and biocompatibility. These alloys enhance the quality and longevity of human life by replacing or treating various parts of the body. However, as these materials are in constant contact with the aggressive body fluids, corrosion of these alloys leads to metal ions release. These ions leach to the adjacent tissues and result in adverse biological reactions and mechanical failure of implant. Surface modifications are used to improve corrosion resistance and biological activity without changing their bulk properties. In this investigation, electropolishing and magnetoelectropolishing were carried out on commercially pure titanium, Ti6Al4V, and Ti6Al4V-ELI. These surface modifications are known to effect surface charge, chemistry, morphology; wettability, corrosion resistance, and biocompatibility of these materials. In vitro cyclic potentiodynamic polarization tests were conducted in phosphate buffer saline in compliance with ASTM standard F-2129-12. The surface morphology, roughness, and wettability of these alloys were studied using scanning electron microscope, atomic force microscope, and contact angle meter, respectively. Moreover, biocompatibility of titanium alloys was assessed by growing MC3T3 pre-osteoblast cells on them.

Keywords biomaterial, corrosion and wear, titanium

1. Introduction

Several degenerative and inflammatory diseases may result in pain and joint stiffness. Primary and secondary osteoarthritis, rheumatoid arthritis (inflammation of synovial membrane), and chondromalacia (softening of cartilage) are the most common diseases of degeneration of synovial joints (Ref 1). These diseases trigger the degenerations of the bones, joints, and other tissues with excruciating pain. To achieve pain relief and improve mobility, the degenerated natural surfaces are replaced with advanced orthopedic biomaterials (Ref 2). Surgical implantation is one of the solutions for restoring the function of the impaired tissues (Ref 3).

Various classes of materials such as metals, polymers, ceramics, and composites have been widely used to restore the structure and function of hard tissues (Ref 4). Metallic materials are commonly used for implantation in the form of plates, pins, and fixing screws for fractured bones. Moreover, metallic implants are also used as parts for total hip prostheses and as femoral and tibia components in total knee arthroplasty (Ref 5). The essential properties of metallic biomaterials are corrosion resistance, low toxicity, and antibacterial nature (Ref 6). Cobalt-chromium and 316L stainless steel have proven to be somewhat biocompatible to the human body (Ref 2), but recent studies shows that titanium alloys are far more superior (Ref 7-12).

Titanium alloys such as commercially pure titanium (CPTi), Ti6Al4V, and Ti6Al4V-ELI are extensively used as surgical implant materials due to their superior mechanical properties (Ref 11), high corrosion resistance, and relatively good biocompatibility (Ref 12, 13). The high corrosion resistance of titanium alloys is due to passive oxide film on their surface. Fortunately, extremely low solubility of the oxides and hydroxides makes it more stable (Ref 12). This film consists of amorphous and non-stoichiometric oxide mixture of rutile, anatase, and brokite (Ref 14). Sometimes, this passive film consists of inclusion and discontinuity spots, which makes the implants more susceptible to corrosion (Ref 12). Owing to the oxide film, these alloys are classified as biologically inert and remain unchanged for long time when implanted into human bodies.

The tissue fluid contains amino acid, dissolved oxygen, chloride, and hydroxyl ions which provide corrosive environment for titanium implants and challenge the biocompatibility and implant durability (Ref 15). Biocompatibility of the implantable material is foremost requirement that the material is acceptable to human body and should not cause any adverse reactions, i.e., allergy, infection, inflammation, and cytotoxicity (Ref 16).

The corrosion of metallic implant is influenced by biological fluids is critical because it can effect the biocompatibility and mechanical integrity (Ref 17). The physiological environment in the human body consists of various elements namely, physical and chemical environments, cells and cellular matrices, tissue fluids, and blood circulatory systems (Ref 18). The chemical environment within the body is controlled by the body fluids. Various body fluids differ significantly in physical

Zia ur Rahman, Luis Pompa, and **Waseem Haider,** Department of Mechanical Engineering, University of Texas Pan American, 1201 W University Dr., Edinburg, TX 78539. Contact e-mail: haiderw@utpa.edu.

properties and composition (Ref 19). Physical (temperature, viscosity, and density) and chemical environment in the body are inter-related. Changes in physical environment affect the chemical environment, which then influences corrosion and biocompatibility of implant (Ref 20). These fluids are buffered saline having a temperature of 37 °C and pH of 7-7.4 under normal conditions (Ref 21). The chemical reactions, biological environment, its pH, and temperature are responsible for corrosion and the dissolution of the surface oxide layer. Extensive release of ions from prosthesis can result in adverse biological reactions which can lead to the mechanical failure of the device (Ref 22). Metal ions release to the adjacent tissues may cause long-term complications. This reduces service life of the implant and increases the chances of the revision surgery.

In this investigation, the electropolishing (EP) and magneto-electropolishing (MEP) surface modifications of CPTi, Ti6Al4V, and Ti6Al4V-ELI were carried out. Each surface modification effects surface roughness, surface chemistry, increases its resistance to corrosion, and enhances biocompatibility.

2. Materials and Methods

2.1 Sample Preparation

CPTi, Ti6Al4V, and Ti6Al4V-ELI rods of medical grade were cut with high-speed saw into circular disks samples having thickness of 0.508×10^{-2} m and diameter of 1.588×10^{-2} m. Samples were grinded with standard metallographic preparation procedures using Buehler® abrasive belt grinder. Tap water was used to clean the debris from samples during abrasive polishing. Each sample was cleaned with deionized water prior to polishing and then ultrasonically cleaned with acetone for 15 min. EP and MEP treatments were performed by Electrobright® (Macungie, PA, USA).

2.2 Material Characterization

The surface morphology of the specimens was analyzed by scanning electron microscope (Carl Zeiss, Germany). The elemental distribution on the surface of each alloy was investigated by energy dispersive spectroscopy (EDS).

Surface roughness of the samples was measured by using atomic force microscope (DI-Veeco, Dimension 3100 USA). Tapping mode which is also called intermittent contact or vibration mode is carried out to conduct high resolution roughness simulations of the surface. Standard Si_3N_4 tips were used for imaging. One specimen of each alloy was analyzed; three individual measurements were made on each specimen. Average roughness (R_a), maximum roughness (R_{max}), skewness (K), and the difference between the maximum and the average surface heights (R_q) were measured.

Kyowa contact angle meter (DM-CE1, Kyowa, Japan) is used for measuring contact angle, surface free energy, and work of adhesion by sessile water drop method. Three chemicals approach (di-water, diiodomethane, and ethylene glycol) were carried out to determine the contact angle, surface free energy, and work of adhesion.

2.3 Electrochemical Analysis

The conventional three-electrode cell was assembled using saturated calomel electrode (SCE) as reference electrode, carbon graphite as counter electrode, and titanium sample as working electrode. The cyclic potentiodynamic corrosion tests were conducted inside the incubator (temperature 37 °C and 5% CO_2) at the scan rate of at 1 mV/s and potential range of −500 to 1500 mV against SCE. The phosphate buffer saline tablets (part # P4417-50TAB Sigma Aldrich® USA) are used to make 1× solution by dissolving one tablet in 200 mL of deionized water. This solution is used as an electrolyte. The chemical composition of the electrolyte solution in g/L is mentioned in Table 1. In order to decrease the concentration of dissolved oxygen and to achieve the de-aerated environment for the corrosion analysis, pure nitrogen (99.9%) gas was purged in the electrolyte for 15 min before each test. The pH and dissolved oxygen concentration is monitored before and after each test.

Gamry potentiostat (reference 600) is used for the cyclic potentiodynamic polarization scans. For the corrosion data analysis, Gamry framework and Gamry Echem Analyst software are used. Corrosion tests were done in compliance with ASTM standard F-2129-12.

2.4 MC3T3 Pre-osteoblast Cell Culture

In order to investigate the effects of surface morphology on the MC3T3 pre-osteoblast cells, the surface of each (untreated and treated) alloy was exposed to these cells. MC3T3-E1 subclone 4 (ATCC® CRL-2593™) cells were first grown in a culture flask. After incubation, 90% confluency was achieved and the cells were trypsinized, centrifuged, and suspended in culture media for further cell seeding.

The cell culture media was prepared by adding 10% fetal bovine serum (FBS) (Thermo Scientific™ HyClone™ SH3008803HI), 1% penicillin streptomycin (Sigma-Aldrich P4333) to MEM alpha from (part # SH4007-13, Thermo scientific, USA). For cell proliferation on metal surface, the special glass cell was used. The sample was fit into the glass cylinder and 30,000 cells for each sample were counted by using hemocytometer. These 30,000 cells were allowed to proliferate on the surface of each sample in order to examine the direct effect of EP and MEP titanium alloys on MC3T3 cells. After 48 h incubation, the media were removed from the cells and cell staining was carried out. For cell staining, the "NucBlue live ready probes reagent" (Hoechst reagent part #33342) from Life Technologies® is used for nucleus while Mitrotraker red (part # M7512), molecular probe of Life Technologies is used for cell mitochondria staining.

3. Results and Discussion

Surface modifications are known to improve surface morphology and chemistry of titanium alloys. Figure 1 shows the SEM photomicrographs and EDS analysis of titanium alloys. SEM photomicrographs reflect that the surface morphologies are significantly changed after EP and MEP. A1, B1, and C1 in Fig. 1 depict the surfaces of untreated alloys, exhibit the abrasive polishing marks on their surfaces. The electropolished CPTi has less uniform morphology and EDS data shows alumina particles incrusted in large pores, while magnetoelectropolised CPTi surface depicts the small pores having titanium oxides. The porous structure is known to effect cell proliferation, provides strong segmentation in bone and good osteointegration (Ref 23).

Table 1 Chemical composition of PBS solution (g/L)

NaCl	Na_2HPO_4	$NaHCO_3$	KCl	KH_2PO_4	$MgSiO_4$	$CaCl_2$
8.0	0.06	0.35	0.4	0.06	0.2	0.14

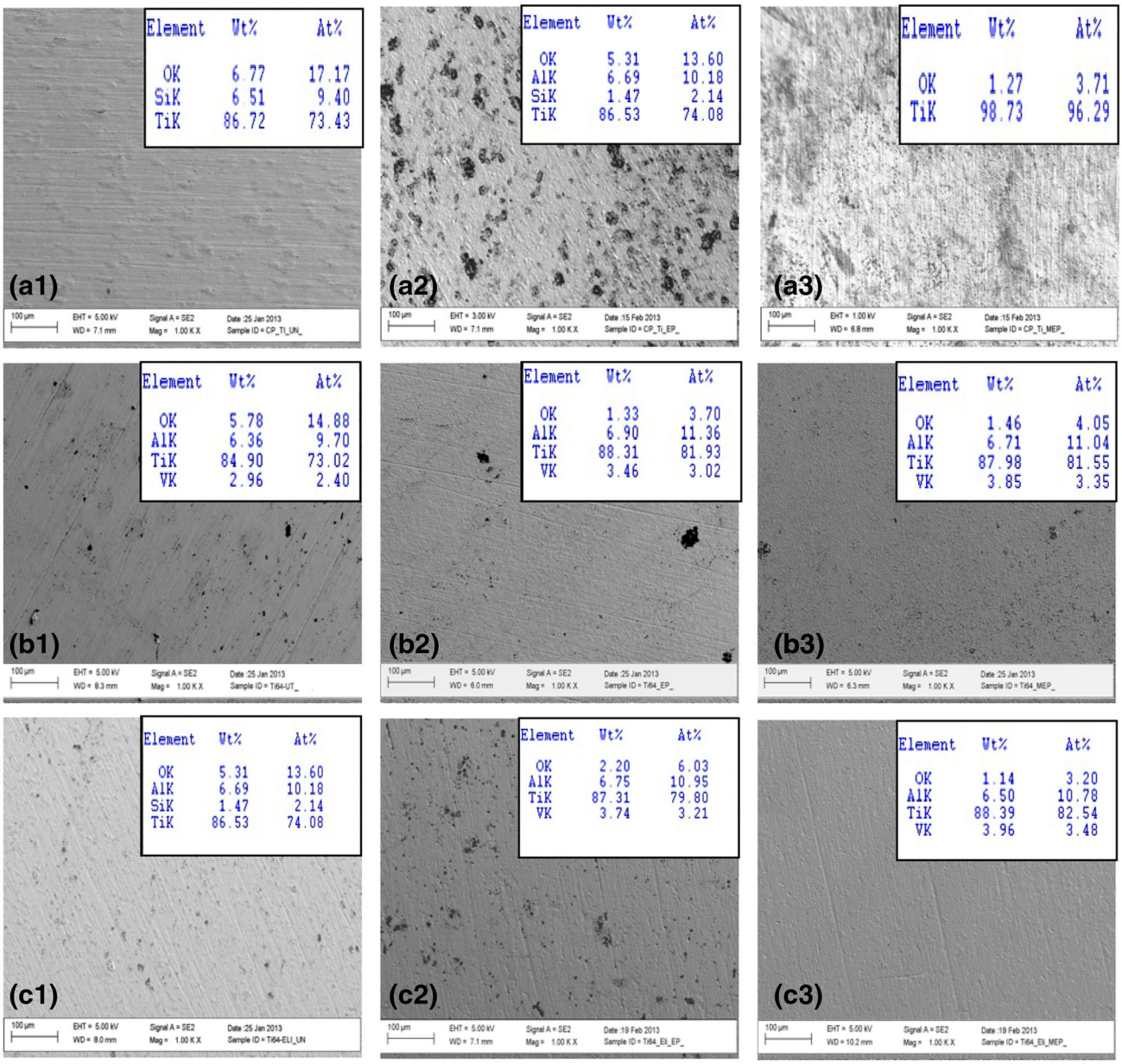

Fig. 1 SEM surface morphology and surface chemistry of the titanium and titanium alloys with different modified surfaces: (A1) CPTi untreated, (A2) CPTi EP, (A3) CPTi MEP; (B1) Ti6Al4V untreated, (B2) Ti6Al4V EP, (B3) Ti6Al4V MEP; (C1) Ti6Al4V-ELI untreated, (C2) Ti6Al4V-ELI EP, (C3) Ti6Al4V-ELI MEP

Magnetoelectropolised Ti6Al4V surface exhibited enhanced microgranular structure as indicated in Fig. 1(B3). By careful observation, electropolished Ti6Al4V surfaces have different surface appearance (less porous) when compared with electropolished CPTi (more porous). Moreover, magnetoelectropolised Ti6Al4V-ELI surface is very smooth when compared with untreated and electropolished Ti6Al4V-ELI.

3.1 Surface Roughness

The integration of the bone tissues to the surface of implant influences the performance of the biomaterial. The imperfect integration of the implant with surrounding tissue results in the failure of implant. From the biomaterial's point of view, main factors contributing to the integration of an implant are the surface topography and surface free energy (SFE) (Ref 24). Studies suggest

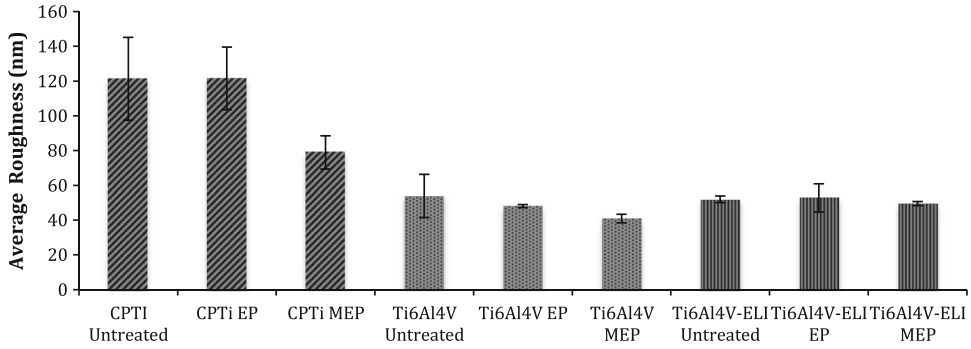

Fig. 2 Average roughness of titanium alloys

that surface roughness influences cell adhesion. Rough surfaces and complex microstructures enhance bone-to-implant contact and result in better osseointegration (Ref 25). The connection between implant and living remodeling bone without any soft tissue component at microscopic level is known as osseointegration (Ref 26). Deligianni et al. have found better cell proliferation and enhanced protein adhesion on rough hydroxyapatite (HA) surface when compared with smooth and polished surface. It was concluded that cell adhesion, proliferation, and detachment strength were sensitive to surface roughness and increased as the roughness of HA increased (Ref 27). The micron and sub-micron scale surface roughness is influential for permanent implants, which have long-term biomechanical integrity of bone-implant interface. The rough surface has positive impact on the osseointegration. It reduces the micro-motions and develops better biomechanical interaction (Ref 28). On the other hand, roughness makes the implants more susceptible to corrosion and initiates pitting in its oxide layer (Ref 29). Optimal mechanical interlocking of implant to the host tissue is required to achieve acceptable integration of implant and tissue.

For comparative analysis, the data of surface average roughness (R_a) are shown in the form of bar graphs in Fig. 2. AFM surface topography of CPTi, Ti6Al4V, and Ti6Al4V-ELI are shown in Fig. 3. The results indicated that in each group of samples the MEP has lowest roughness in comparison with EP and untreated alloys.

3.2 Wettability

Wettability of materials is of significant interest in biomedical application because of its effects on the cell adhesion and cell proliferation. Implants are always in contact with body fluids, these body fluids have great influence on the surface of the implant in the form of protein adsorption, platelet adhesion/activation, cell and bacterial adhesion, and proliferation (Ref 30). Wettable surfaces with low contact angle and higher surface energy are termed as hydrophilic surfaces. However, wettable surfaces with high contact angle and low surface energy are known as hydrophobic surfaces (Ref 31).

The sessile drop method was used to measure wettability by employing three solvents: DI-water (mild polar), ethylene glycol (neutral), and diiodomethane (highly polar). The test was performed per solvent on each specimen at a location separated by sufficient spacing in order to prevent the potential influence of previous tests. According to Young-Dupree equation, the contact angle (θ) can be expressed as

$$\gamma_{lg}^{\cos\theta} = \gamma_{sg} + \gamma_{sl},$$

where γ_{sg} is the surface energy of the solid, γ_{sl} is the solid liquid interfacial energy, and γ_{lg} is the surface energy of the liquid. Famas analysis software was used to evaluate the surface free energy (SFE) by using the following equation:

$$\gamma^{\text{total}} = \gamma^{\text{d}} + \gamma^{\text{p}} + \gamma^{\text{h}}$$

γ^{total} is the total surface free energy, γ^{d} is the SFE dispersion component γ^{p}, is the SFE polar component, and γ^{h} the SFE hydrogen bond.

Five drops of each liquid on each samples were analyzed and the average SFE was calculated.

In case of the CPTi, the contact angle shows significant increase after EP and MEP. These surface treatments change the surface chemistry which is obvious from EDS data. The content of oxygen is decreased as shown in Fig. 1. This decrease in the oxygen content changes the polar movement of the molecules of water droplet on the surface of the substrate which effects the orientation of molecule and drop behavior with the solid surface. Figure 5 shows the wetting ability of Ti6Al4V. The contact angle of electropolished surface is high but it shows the significant decrease in magnetoelectropolished surface. However, Ti6Al4V-ELI magnetoelectropolished surface is more hydrophobic. Roughness of the surface also effect the contact angle. The rough surface provides large contact area to the drop in comparison with smoother surface and has great influence on the wettability of the surface (Ref 32).

Surface free energy (SFE) is inversely proportional to contact angle and guides the first events occurring at the biomaterial/biological interface, such as interaction of water and proteins with biomaterial (Ref 33). However, the measurement of surface energy estimation from contact angle is a hard task because biomaterial surfaces are always rough and/or heterogeneous (Ref 25). Wettability is strongly influenced by surface roughness and surface chemistry (Ref 34). It has been observed that the contact angle is influenced more by the microscopic inclusions and discontinuities than by interfacial energetics and cause hysteresis if $R_a \geq 0.1$ μm (Ref 32). However, surface energy estimation is temperature sensitive and just requires thermodynamically significant angles. Moreover, surface roughness, wettability, and cell interaction properties are inter-related phenomenon, and have counter effects on each other. Their relation is complex and needs further investigation.

Figure 4, 5, and 6 clearly show that the higher contact angle means lower SFE. The Kitazaki Hata surface energy results indicate the significant changes in surface energetics and adhesion properties as well as contact angle. Young's contact angle shows that the untreated CPTi has lowest contact angle (90°) and its SFE 45 mJ/m while electropolished Ti6Al4V shows the highest contact angle (120°) and lowest SFE (38 mJ/m). Similarly magnetoelectropolished Ti6Al4V-ELI has lowest contact angle with the highest SFE as depicted in Fig. 6.

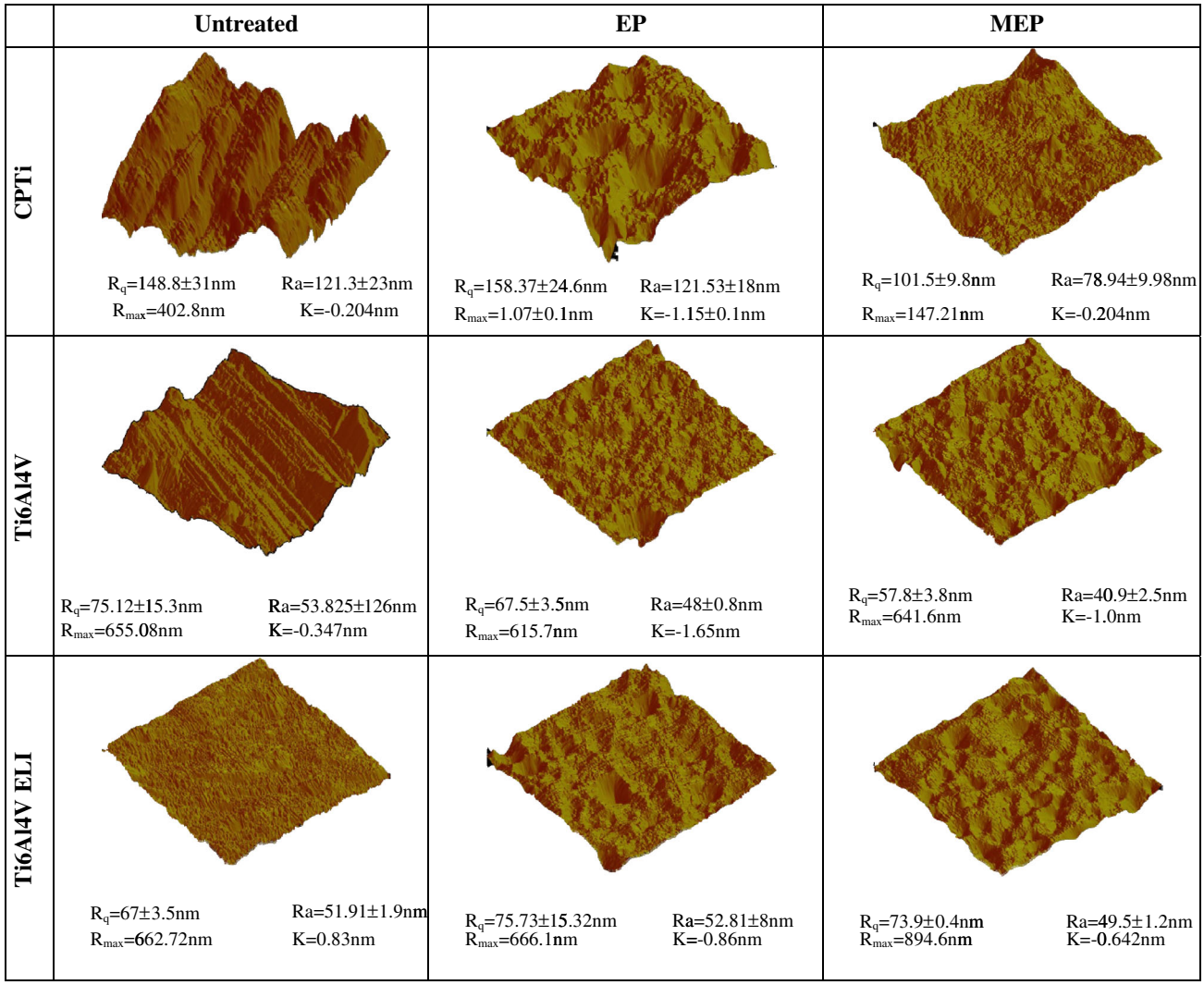

Fig. 3 AFM 3D simulation of roughness of untreated, EP, and MEP surfaces. R_p is root mean square of roughness, R_a shows arithmetic mean of roughness, R_{Max} is maximum peak height, and K is skewness

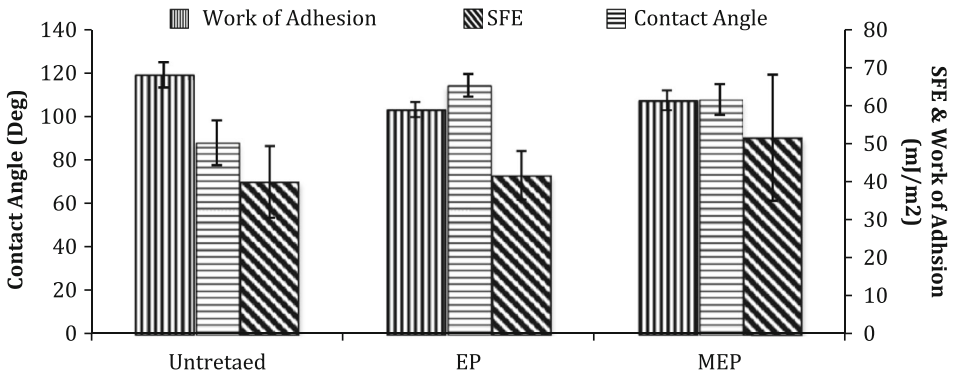

Fig. 4 Kitazaki Hata average values of CPTi

The oxide layer on surface has great influence on the polar bonds and their interaction with water and aminoacids. Studies have also reveal that lower SFE values correspond to favorable cellular adhesion and cell activities (Ref 35). Ponsonnet et al. (Ref 36) investigated that 30-40 mJ/m^2 SFE corresponds to higher cell proliferation and indicated inflecting points in the mentioned range. Cell adhesion is an important term for successful implantation. Better cell adhesion results in strong osseointegration. In orthopedics and trauma surgery, the success of implants surgery is based on osseointegration. It is generally noticed that hydrophilic surface the cell adhesion is more stable when compared to hydrophobic surface. The

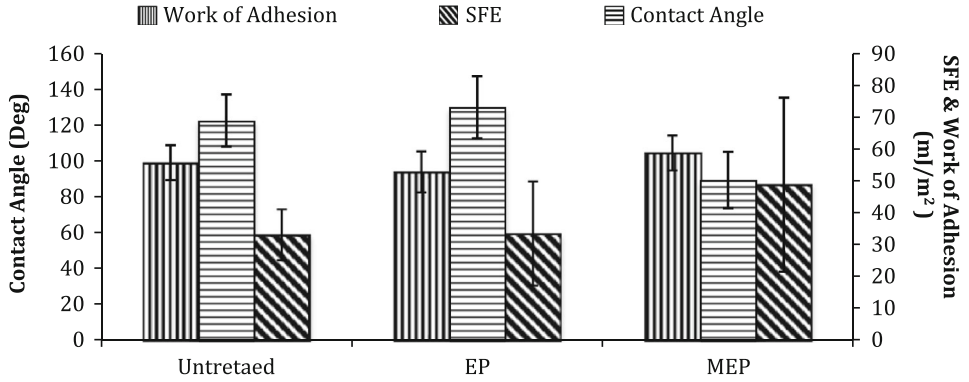

Fig. 5 Kitazaki Hata average values of Ti6Al4V

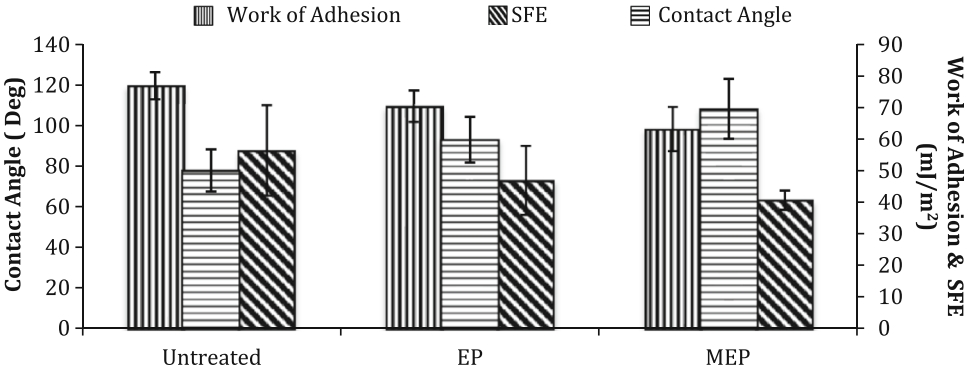

Fig. 6 Kitazaki Hata average values of Ti6Al4V-ELI

hydrophilic surface provides good osseointegration and more mechanically stable thus the chances of loosing implant are smaller (Ref 37). SFE and hydrophilicity of implant surfaces may be especially important during initial conditioning by proteins and during initial cell adhesion. Researchers found that the thrombogenicity of a material's surface increases with increasing surface energy (Ref 32).

3.3 Potentiodynamic Polarization Scans

Metallic implants exhibit corrosion when in contact with body fluid due to the presence of chloride ions and proteins. Various chemical reactions take place on the surface of implant inside the body. The rate of attack of general corrosion is very low due to the passive oxide layer on implant surface. Crevice and pitting corrosion are the most common types of corrosion that takes place in metallic implants (Ref 38). Most of the medical implant especially orthopedics implants or load-bearing implants are subjected to low cyclic loadings, e.g., hip implant is subjected to cyclic loading which causes the fatigue corrosion and fretting corrosion. The pH of the environmental is also an important factor and has great influence on corrosion of metallic implants (Ref 39).

The corrosion of the titanium implants has great influence on passive oxide film. The oxide film makes the implant resistant to corrosion and considerably reduces the corrosion rate. Generally, oxide layer is thermodynamically unstable at negative voltages and pH has great influence on it. According to the Cabrera and Mott, the oxide film on any metals surface

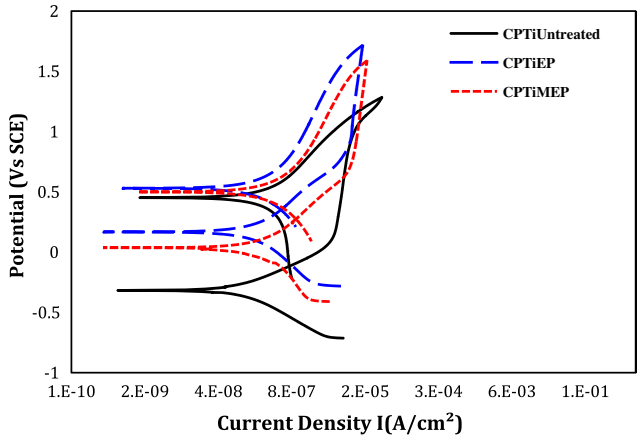

Fig. 7 Cyclic polarization scans of CPTi

can be altered by applying electric field and voltage difference at the interface, the oxide layer became thermodynamically unstable at negative voltage and at lower pH and this results in the dissolution of the oxide layer (Ref 40), thus the corrosion resistance is greatly dependent on alloying elements and their oxide film. The corrosion of implants lead to implant fracture. The abrasion of metal oxide and corrosion generates ionic and particulate debris and their deposition in the local tissue cause potential toxicities associated with the elements used in the implant alloys. Therefore, the stability of the oxide layer is a major requirement in the implant materials.

Cyclic polarization technique can be used to understand the stability of titanium implants in a specific environment. This is a highly useful method for determining the susceptibility of metals to pitting when placed in a specific corrosive environment. Potentiodynamic cyclic polarization measurements were used to determine the active-passive characteristics of samples before and after surface treatment. The polarization scans of each alloy, before and after surface treatments are given in Fig. 7, 8, and 9.

From the polarization scan of each sample, no hysteresis loop is observed and all the scans have same general features of active, passive, and trans-passive regions. In general, the pitting and crevice corrosion can be evaluated based on the formation of a loop and an evaluation of the sample can be made based on the area of loops that form in the cyclic polarization curves. The higher the loop area, the greater is the tendency toward pitting and crevice corrosion. In all cases, the reverse scan takes entirely different path, which is clear indication of resistance to pitting and crevice corrosion. However, to be more precise the Tafel extrapolation method was carried out to calculate the corrosion rates and E_{corr} values and are displayed in Table 2.

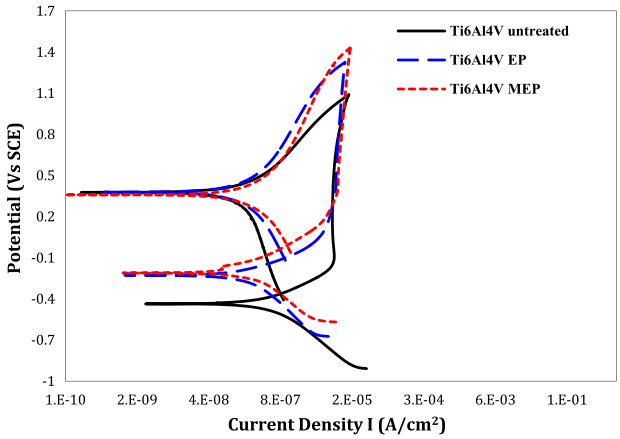

Fig. 8 Cyclic polarization scans of Ti6Al4V

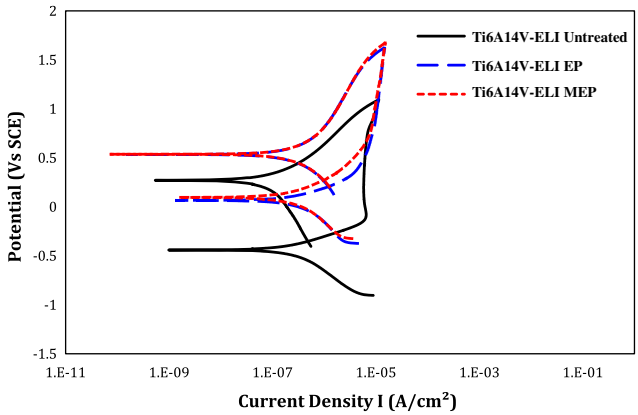

Fig. 9 Cyclic polarization scans of Ti6Al4V-ELI

In case of CPTi (Fig. 7), the maximum corrosion rate was observed for untreated alloys. There is no significant difference in I_{corr} values of untreated and surface-treated alloys of CPTi. However, EP and MEP titanium alloys behave noble and E_{corr} is shifted to positive potential. The E_{corr} value of CPTi EP is higher than CPTi MEP while CPTi untreated E_{corr} value is very low in comparison. The lower E_{corr} indicates that untreated CPTi is more susceptible to corrosion. The E_{corr}, I_{corr}, and corrosion rates are displayed in Table 2. E_{corr} of reverse scan is always above the E_{corr} of forward scan, which shows the passivation and resistance to corrosion. On the other hand, EP and MEP have the same effects on Ti6Al4V and Ti6Al4V-ELI as shown in Fig. 8 and 9, respectively. Both of these alloys are showing more passive behavior after surface modification of EP and MEP. EP and MEP shift the alloys to more noble potentials and make them more resistant to crevice and pitting corrosion. The corrosion curves depict that after EP and MEP treatments the corrosion potential and current densities have been improved. Moreover, it is also shown that the Ti6Al4V is less passivized when compared to Ti6Al4V-ELI. Ti6Al4V-ELI MEP is significantly more passivized when compared with other titanium alloys.

3.4 Cell and Surface Interaction

Cell adhesion is the initial interaction with an implant surface followed by spreading, which forms the basis for proliferation. Initially, cells do not communicate directly with the implant, but are guided to sites by biological interactive molecules. This interaction results in the formation of either a fibrous tissue or a bond. The protein adhesion has great influence on the surface chemistry and surface energetics. Wettability studies and roughness data suggested that each alloy has different values and thus cell proliferation on these surfaces must be different. In order to understand the cell-biomaterial interaction, cells were allowed to proliferate. Figure 10 exhibits MC3T3 cells on titanium alloys after 3 days of incubation. Excellent cell proliferation was observed on Ti6Al4V MEP surface in comparison with untreated and EP

Table 2 Cyclic polarization data

Sample	Area (cm^2)	Dissolved oxygen (mg/L)	pH before test	pH after test	E_{corr} (mV)	I_{corr} (A/cm^2)	E_V	Corrosion rate (mm/year)
CPTi Untreated	1.282	0.8	7.20	7.00	−317.0	64.40E−9	1.285	5.50E−04
CPTi EP	1.282	0.8	7.10	7.02	197.0	43E−9	1.715	3.72E−04
CPTi MEP	1.282	0.7	7.21	7.20	6.65	10E−9	1.589	8.66E−05
Ti6Al4V Untreated	1.282	1.7	7.21	7.10	−437	159E−9	1.090	1.39E−03
Ti6Al4V EP	1.282	1.6	7.24	7.10	−228	115E−9	1.325	1.01E−03
Ti6Al4V MEP	1.282	1.3	7.28	7.13	−211	18.10E−9	1.430	1.56E−04
Ti64Al4V-ELI Untreated	1.282	1.0	7.20	7.00	−44.7	48.20E−9	1.081	4.24E−04
Ti64Al4V-ELI EP	1.282	0.9	7.21	7.13	47.60	31.40E−9	1.579	2.76E−04
Ti64Al4V-ELI MEP	1.282	1.1	7.25	7.15	114.0	33.70E−9	1.668	2.96E−04

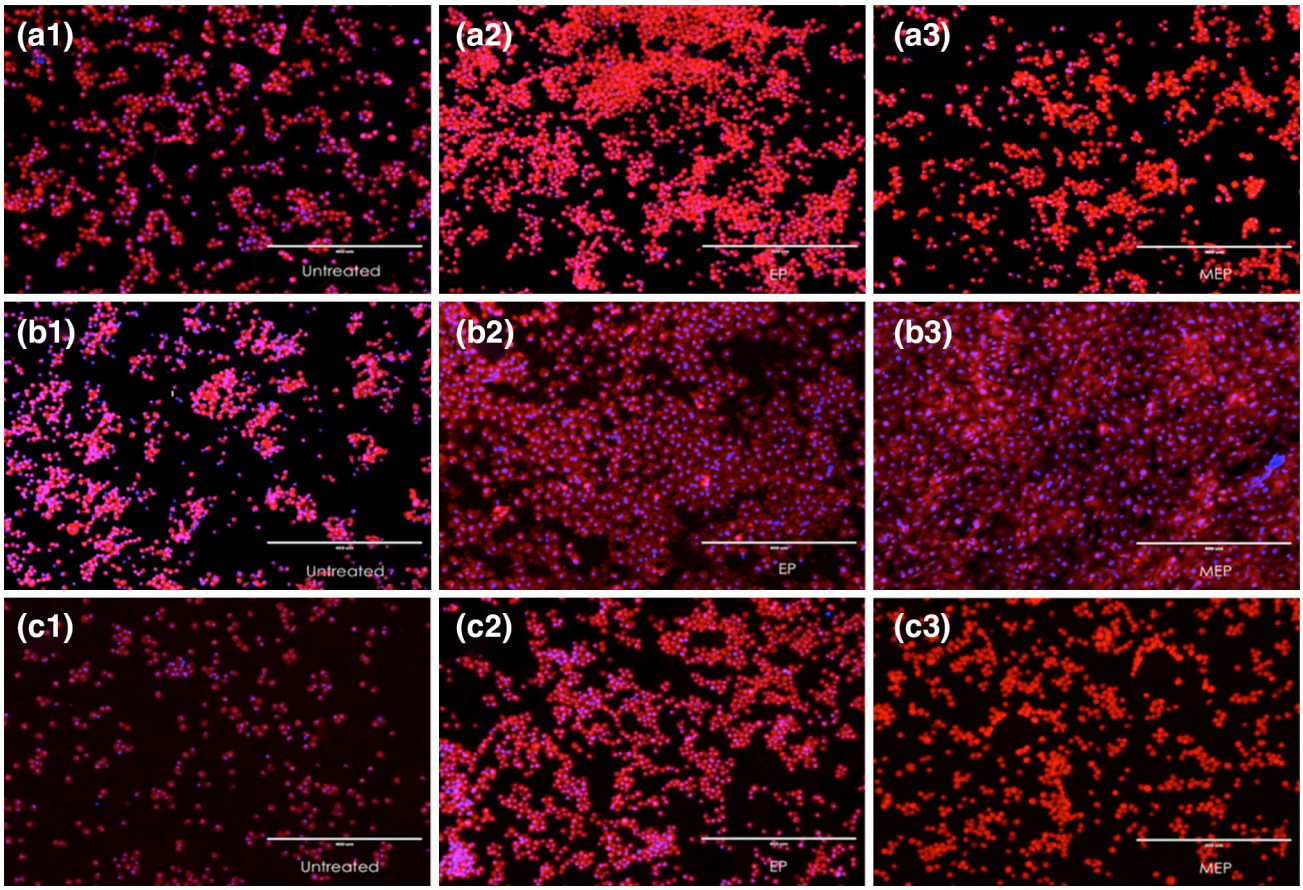

Fig. 10 MC3T3 pre-osteoblast cell proliferation on the surface; (A1) CPTi untreated, (A2) CPTi EP, (A3) CPTi MEP; (B1) Ti6Al4V untreated, (B2) Ti6Al4V EP, (B3) Ti6Al4V MEP; and (C1) Ti6Al4V-ELI untreated, (C2) Ti6Al4V-ELI EP, (C3) Ti6Al4V-ELI MEP

surfaces. The poor cell proliferation is observed on all untreated alloys when compared to EP and MEP alloys. This is probably due to high concentration of leached metals ions from the bare surface.

4. Conclusions

This study indicates that EP and MEP are effective technologies and provide a new podium for osteoblast proliferation. Different surface treatments show different morphologies and topographies along with different surface chemistry. The EDS data indicates that EP and MEP treatments reduce the contents of oxygen at the surface of titanium alloys. EP changes the surface chemistry and surface morphology by providing a porous morphological structure while MEP provides a micro-granular structure.

The wettability studies demonstrate that the surface chemistry has great influence on surface energetics and contact angle. Surface roughness and wettability studies showed that the surface chemistry is playing more dominant role than surface roughness in the wettability of titanium alloys. EP and MEP treatments produced stable oxide passive film on the alloys and increase their resistance to pitting and crevice corrosion in comparison with bare surface. From the cell proliferation experiments, it was concluded that MC3T3 cells were proliferating better on EP and MEP surfaces in comparison with bare surfaces. The MC3T3 osteoblast cell interaction with the titanium and its alloys depicts better cell proliferation.

Acknowledgments

W. Haider would like to acknowledge 2013 Ralph E. Powe Junior Faculty Enhancement Award. Authors would like to acknowledge Dr. Shivani Maffi and Mr. Alfonso Salinas for tissue culture training and SEM, respectively.

References

1. M. Long and H.J. Rack, Titanium Alloys in Total Joint Replacement—A Materials Science Perspective, *Biomaterials*, 1998, **19**(18), p 1621–1639
2. H.J. Rack and J.I. Qazi, Titanium Alloys for Biomedical Applications, *Mater. Sci. Eng. C*, 2006, **26**(8), p 1269–1277
3. A.C. August, C.H. Aldam, and P.B. Pynsent, The McKee-Farrar Hip Arthroplasty. A Long-Term Study, *J. Bone Joint Surg. Br.*, 1986, **68**, p 520–527
4. F.J. Schoen, J.E. Lemons, B.D. Ratner, A.S. Hoffman, B.D. Ratner, A.S. Hoffman, F.J. Schoen, and J.E. Lemons, *Biomaterials Science: An Introduction to Materials in Medicine*, 3rd ed., Academic Press, Waltham, 2001, p 35–42
5. L. Trentani, F. Pelillo, F.C. Pavesi, L. Ceciliani, G. Cetta, and A. Forlino, Evaluation of the $TiMo_{12}Zr_6Fe_2$ Alloy for Orthopaedic Implants: In Vitro Biocompatibility Study by Using Primary Human Fibroblasts and Osteoblasts, *Biomaterials*, 2002, **23**, p 2863–2869
6. B. Li and B.E. Logan, Bacterial Adhesion to Glass and Metal-Oxide Surfaces, *Colloids Surf. B*, 2004, **36**, p 81–90

7. G. Manivasagam, D. Dhinasekaran, and A. Rajamanickam, Biomedical Implants: Corrosion and Its Prevention—A Review, *Recent Pat. Corr. Sci.*, 2010, **2**, p 40–54
8. B. Al-Mangour, R. Mongrain, E. Irissou, and S. Yue, Improving the Strength and Corrosion Resistance of 316L Stainless Steel for Biomedical Applications Using Cold Spray, *Surf. Coat. Technol.*, 2013, **216**, p 297–307
9. Y. Tanaka, H. Saito, Y. Tsutsumi, H. Doi, H. Imai, and T. Hanawa, Active Hydroxyl Groups on Surface Oxide Film of Titanium, 316L Stainless Steel, and Cobalt-Chromium-Molybdenum Alloy and Its Effect on the Immobilization of Poly(ethylene glycol), *Mater. Trans.*, 2008, **49**, p 805–811
10. J.B. Shamsul, A.Z. Nurhidayah, and C.M. Ruzaidi, Characterization of Cobalt-Chromium-HAP Biomaterial for Biomedical Application, *J. Appl. Sci. Res.*, 2007, **3**, p 1544–1553
11. M. Niinomi, Mechanical Properties of Biomedical Titanium Alloys, *Mater. Sci. Eng. A*, 1998, **243**(1–2), p 231–236
12. T. Hryniewicz, R. Rokicki, and K. Rokosz, Magnetoelectropolished Titanium Biomaterial, *Surf. Coat. Technol.*, 2009, **203**(10–11), p 1508–1515
13. C. Oldani, A. Dominguez, and T. Eli, Titanium as a Biomaterial for Implants, *Recent Advances in Orthoplasty*, S.K. Fokter, Ed., InTech, Rijeka, 2012
14. S. Roessler, R. Zimmermann, D. Scharnweber, C. Werner, and H. Worch, Characterization of Oxide Layers on Ti6Al4V and Titanium by Streaming Potential and Streaming Current Measurements, *Colloids Surf. B*, 2002, **26**, p 387–395
15. S. Bauer, P. Schmuki, K. von der Mark, and J. Park, Engineering Biocompatible Implant Surfaces, *Prog. Mater. Sci.*, 2013, **58**(3), p 261–326
16. A. Cremasco, A.D. Messias, A.R. Esposito, E.A.D.R. Duek, and R. Caram, Effects of Alloying Elements on the Cytotoxic Response of Titanium Alloys, *Mater. Sci. Eng. C*, 2011, **31**(5), p 833–839
17. I. Gurappa, Characterization of Different Materials for Corrosion Resistance Under Simulated Body Fluid Conditions, *Mater. Charact.*, 2002, **49**(1), p 73–79
18. S. Virtanen, I. Milosev, E. Gomez-Barrena, R. Trebse, J. Salo, and Y.T. Konttinen, Special Modes of Corrosion Under Physiological and Simulated Physiological Conditions, *Acta Biomater.*, 2008, **4**, p 468–476
19. R. Schenk, *Titanium in Medicine: Material Science, Surface Science, Engineering, Biological Responses, and Medical Applications*, Springer, New York, 2001, pp. 145–168
20. T. Hanawa, K. Asami, and K. Asaoka, Repassivation of Titanium and Surface Oxide Film Regenerated in Simulated Bioliquid, *J. Biomed. Mater. Res.*, 1998, **40**, p 530–538
21. A. Oyane, H.-M. Kim, T. Furuya, T. Kokubo, and T. Nakamura, Preparation and Assessment of Revised Simulated Body Fluids, *J. Biomed. Mater. Res. A*, 2003, **65**, p 188–195
22. M.A. Khan, R.L. Williams, and D.F. Williams, In-Vitro Corrosion and Wear of Titanium Alloys in the Biological Environment, *Biomaterials*, 1996, **17**, p 2117–2126
23. H. Shen and L.C. Brinson, A Numerical Investigation of Porous Titanium as Orthopedic Implant Material, *Mech. Mater.*, 2011, **43**(8), p 420–430
24. F. Rupp, L. Scheideler, N. Olshanska, M. de Wild, and J. Geis-Gerstorfer, Enhancing Surface Free Energy and Hydrophilicity Through Chemical Modification of Microstructured Titanium Implant Surfaces, *J. Biomed. Mater. Res. A*, 2006, **76**, p 323–334
25. J.I. Rosales-Leal et al., Effect of Roughness, Wettability and Morphology of Engineered Titanium Surfaces on Osteoblast-Like Cell Adhesion, *Colloids Surf. A*, 2010, **365**, p 222–229
26. P.I. Brånemark, Osseointegration and Its Experimental Background, *J. Prosthet. Dent.*, 1983, **50**, p 399–410
27. D.D. Deligianni, N.D. Katsala, P.G. Koutsoukos, and Y.F. Missirlis, Effect of Surface Roughness of Hydroxyapatite on Human Bone Marrow Cell Adhesion, Proliferation, Differentiation and Detachment Strength, *Biomaterials*, 2001, **22**, p 87–96
28. J.E. Feighan, V.M. Goldberg, D. Davy, J.A. Parr, and S. Stevenson, The Influence of Surface-Blasting on the Incorporation of Titanium-Alloy Implants in a Rabbit Intramedullary Model, *J. Bone Joint Surg. Am.*, 1995, **77**, p 1380–1395
29. R.B. Alvarez, H.J. Martin, M.F. Horstemeyer, M.Q. Chandler, N. Williams, P.T. Wang, and A. Ruiz, Corrosion Relationships as a Function of Time and Surface Roughness on a Structural AE44 Magnesium Alloy, *Corros. Sci.*, 2010, **52**, p 1635–1648
30. L.-C. Xu and C.A. Siedlecki, Effects of Surface Wettability and Contact Time on Protein Adhesion to Biomaterial Surfaces, *Biomaterials*, 2007, **28**, p 3273–3283
31. J.Y. Lim, M.C. Shaughnessy, Z. Zhou, H. Noh, E.A. Vogler, and H.J. Donahue, Surface Energy Effects on Osteoblast Spatial Growth and Mineralization, *Biomaterials*, 2008, **29**, p 1776–1784
32. W. Haider, Enhanced Biocompatibility of NiTi (Nitinol) Via Surface Treatment and Alloying," FIU Electronic Theses and Dissertations, Paper 177, 2010
33. K. Kieswetter, Z. Schwartz, T.W. Hummert, D.L. Cochran, J. Simpson, D.D. Dean, and B.D. Boyan, Surface Roughness Modulates the Local Production of Growth Factors and Cytokines by Osteoblast-Like MG-63 Cells, *J. Biomed. Mater. Res.*, 1996, **32**, p 55–63
34. G.B. Sigal, M. Mrksich, and G.M. Whitesides, Effect of Surface Wettability on the Adsorption of Proteins and Detergents, *J. Am. Chem. Soc.*, 1998, **120**, p 3464–3473
35. B. Feng, J. Weng, B.C. Yang, S.X. Qu, and X.D. Zhang, Characterization of Surface Oxide Films on Titanium and Adhesion of Osteoblast, *Biomaterials*, 2003, **24**, p 4663–4670
36. L. Ponsonnet, K. Reybier, N. Jaffrezic, V. Comte, C. Lagneau, M. Lissac, and C. Martelet, Relationship Between Surface Properties (Roughness, Wettability) of Titanium and Titanium Alloys and Cell Behaviour, *Mater. Sci. Eng. C*, 2003, **23**, p 551–560
37. L. Le Guéhennec, A. Soueidan, P. Layrolle, and Y. Amouriq, Surface Treatments of Titanium Dental Implants for Rapid Osseointegration, *Dent. Mater.*, 2007, **23**, p 844–854
38. Z. Ahmad, *Principles of Corrosion Engineering and Corrosion Control*, Wiley Canada, Limited, Mississauga, 1999, p 271–351
39. M. Geetha, A.K. Singh, R. Asokamani, and A.K. Gogia, Ti Based Biomaterials, the Ultimate Choice for Orthopaedic Implants—A Review, *Prog. Mater Sci.*, 2009, **54**(3), p 397–425
40. V.P. Zhdanov and B. Kasemo, Cabrera-Mott Kinetics of Oxidation of nm-Sized Metal Particles, *Chem. Phys. Lett.*, 2008, **452**, p 285–288